Supplementary Information for

Air-stable and Lithium-compatible Garnet Pellet Enabled by Surface Doping for High Performance Solid-state Batteries

Sijie Guo,[a] Ting-Ting Wu,[a] Si-Qi Lu,[ab] Su-Ting Weng,[c] Mu-Yao Qi,[ab] Bing Li,[ab] Yong-Gang Sun,[d] Si-Dong Zhang,[ab] Xue-Feng Wang,[c] Hong-Shen Zhang,[ab] and An-Min Cao* [ab]

Experimental Section/Methods

Synthesize of LLZT pellets:

Garnet-type solid-state electrolytes (SSEs) in the form of LLZT pellets were synthesized using a conventional solid-state reaction method[5], following procedures reported in prior studies. Stoichiometric amounts of $LiOH•H_2O$ (≥98%, Aladdin), La_2O_3 (99.99%, Macklin), ZrO_2 (99.99%, Aladdin), and Ta_2O_5 (99.99%, Macklin) were ball-milled (PM 100, Retsch) at 300 rpm for 6 h in a zirconia ceramic vial with 2-propanol (Chromatographically pure). To compensate for Li loss during high-temperature sintering, 10 wt.% excess $LiOH•H_2O$ was added. The mixed powder underwent calcination at 900 °C for 6 h to produce LLZT powder. Subsequently, the LLZT powder was ball-milled at 300 rpm for 6 h with 2-propanol, pressed into pellets under an isostatic pressure of 350 MPa, and sintered at 1140 °C for 16 h. The acquired LLZT pellets are sliced into thinner pieces approximately 500 μm thick using a low-speed diamond saw (SYJ-150, HF-Kejing). Subsequently, the garnet electrolyte ceramic discs undergo polishing with SiC abrasive papers, initially using 800 grit followed by 1500 grit. Finally, the discs are further polished inside a glovebox filled with pure Ar using 2000 grit SiC abrasive papers, ensuring precise control to achieve a final thickness of approximately 400 μm. The resulting LLZT discs are stored in a glove box (O_2 < 0.1 ppm and H_2O < 0.1 ppm) for further use.

Synthesize of $Li_5Fe_{0.5}La_3Zr_{1.5}Ta_{0.5}O_{12}$:

Garnet-type solid-state electrolytes (SSEs) in the form of LLZT pellets were synthesized using a conventional solid-state reaction method[5], following procedures reported in prior studies. Stoichiometric amounts of $LiOH•H_2O$ (≥98%, Aladdin), La_2O_3 (99.99%, Macklin), ZrO_2 (99.99%, Aladdin), Ta_2O_5 (99.99%, Macklin) and Fe_2O_3 (99%, Aladdin)were ball-milled (PM 100, Retsch) at 300 rpm for 6 h in a zirconia ceramic vial

with 2-propanol (Chromatographically pure). To compensate for Li loss during high-temperature sintering, 10 wt.% excess $LiOH•H_2O$ was added. The mixed powder underwent calcination at 900 °C for 6 h to produce LLZT powder. Subsequently, the LLZT powder was ball-milled at 300 rpm for 6 h with 2-propanol, pressed into pellets under an isostatic pressure of 350 MPa, and sintered at 1140 °C for 16 h.

Preparation of Fe_2O_3 nanofilm on ZrO_2:

In a standard solution-based approach for Fe_2O_3 nanofilms, 50 mM $Fe(NO_3)_3$ (99.9%, Aladdin) and 50 mg/mL PAA (1.8k, Aladdin) are dissolved in isopropanol (IPA) to create a red and transparent precursor solution. A 30 μL precursor solution is dripped onto a ZrO_2 wafer (1 cm × 1 cm), and a spin-coating process is conducted with key parameters set at 5000 rpm for 30 s using a Laurell spin-coater (EDC-650Mz-23NPPB) at room temperature. The polymer-$Fe(NO_3)_3$ layer is then deposited on the ZrO_2 wafer. Subsequently, the modified wafer is transferred into a tube furnace for a sintering process at 650 °C with an increasing rate of 5 °C/min in an oxygen atmosphere for 10 min. After pyrolysis, 4 nm Fe_2O_3 nanofilms are formed on the ZrO_2 wafer surface. The thickness of Fe_2O_3 nanofilms can be modulated by changing the concentrations of $Fe(NO_3)_3$ and PAA as the following listed:

Concentration of $Fe(NO_3)_3$	Concentration of PAA	Thickness of Fe_2O_3
25 mM	25 mg/mL	2 nm
50 mM	50 mg/mL	4 nm
100 mM	100 mg/mL	10 nm

Preparation of CF-LLZT pellets:

To form on CF-LLZT pellets, 30 μL precursor solution containing 50 mM $Fe(NO_3)_3$ and 50 mg/mL PAA is spin-coated onto one side of the prepared LLZT pellets by using the above-introduced film-construction technique. The same process is repeated to modify another side of LLZT pellets. This LLZT pellet is then transferred into a tube furnace for a sintering process. The pyrolysis temperature is elevated to 750 °C at a heating rate of 5 °C/min. After two hours, it is naturally cooled down to room

temperature. The whole process is carried out in an oxygen atmosphere. After that, the CF-LLZT pellets are transferred into an Ar-filled glove box immediately and stored for the next usage.

Battery Assembly and electrochemical measurements

All process of cells assembly/disassembly is performed in an Ar-filled glove box with H_2O and O_2 contents below 0.1 ppm.

Symmetric Battery Assembly:

CF-LLZT pellets are sandwiched by two identical fresh lithium foil discs (0.9 cm in diameter and 0.3 mm thick). The stacked Li/CL-LLZT/Li is preheated at 170 °C for 5 min with the pressure of ~0.03 Pa, and the temperature is then elevated to 300 °C for another 15 min. After cooling down to room temperature, the thin lithium foil discs become stuck onto the surface of pellets. Then the Li/CF-LLZT/Li with flexible nickel foams is assembled in a standard CR2032 coin cell. All the LLZT pellets we used as control samples has been heated at 750 °C before their electrochemical test. The pristine LLZT pellets are heated with lithium foil discs via the same procedure and assembled with Ni foam in a standard CR2032 coin cell. The charge/discharge cycling of the coin cells is tested by using a LAND CT2001A battery test system.

Full Battery Assembly:

The cathode is prepared by blending the active materials of either NMC0.83 or $LiFePO_4$ with the conductive agent (Super P) and the binder (polyvinylidene fluoride, PVDF) in a weight ratio of 8: 1: 1. N-Methyl-2-pyrrolidone (NMP) is added as the viscosity regulator to form a slurry by means of a rotary mixer (Mazerustar KK-400WE). Then, the slurry is painted onto the aluminum foil and transferred into a vacuum furnace at 80 °C for drying (10 h). The above foil is punched into round disks with 0.7 cm in diameter for its usage as cathode electrodes. The loading of the active material is at a value of about 4.8 mg cm^{-2}.

LLZT and CF-LLZT pellets are used as electrolytes in the full battery assembly. For the anode end, good contact between Li and CF-LLZT is constructed via a process as described above for symmetrical battery assembly while keeping the other side of the pellet clean. The prepared cathode electrode is then covered on the unmodified side

of this CF-LLZT pellet to build the full cell in a typical CR2032 cell case. All cells including symmetric batteries and full batteries are encapsulated at the pressure of 25 kg cm^{-2} (not the actual pressure in cells) with a highly conductive Ni foam and the inner pressure of cells is not controlled. A tiny amount of SN electrolyte (0.5 M LiTFSI dissolved in SN) is added onto the cathode side for a full battery test. The electrochemical measurements are performed on a LAND CT2001A battery test system at a constant temperature of 25 °C.

Materials characterization:

A JEOL-F200 transmission electron microscope (TEM) with an accelerating voltage of 200 kV is adopted to obtain the TEM images, EDS and EELS signals. Preparation of TEM specimen: The lamellar TEM specimen is prepared by a standard"lift-out technique" using an FEI Helios dual scanning electron beam/focused ion beam system on Helios NanoLab 600i (Thermo Fisher Scientific). For the purpose of minimizing the Ga-ions beam damage, a protective carbon layer is deposited on the surface of the specimen using a Carbon Coater (LEICA EM ACE600) prior to FIB process. D8 Bruker Advance diffractometer with Cu Kα radiation (λ = 1.54060 Å) is used to obtain the X-ray diffraction (XRD) patterns. ToF-SIMS V instrument (ION-TOF GmbH, Münster, Germany) is selected to measure the time-of-flight secondary-ion mass spectrometry (ToF-SIMS) with Cs^+ primary ion beam and the data were recorded in ultrahigh vacuum at a pressure of 10^{-9} Torr in a negative model. Raman Spectra and Raman mapping (HORIBA LabRAM HR Evolution, France) are used to analyze the Li_2CO_3 distribution on SSEs surface. For the study of the surface wettability, the pellets of both Li/LLZT and Li/CF-LLZT are firstly fractured for a clear SEM observation on the cross-sections by a scanning electron microscope (Hitachi S-4800, Japan). The Electrochemical impedance spectroscopy (EIS) measurements are performed on a Metrohm Autolab workstation (Muti Autolab M204) with an alternating current amplitude of 10 mV and a frequency range from 10.0 MHz to 0.1 Hz. To determine the ionic conductivity of the LLZT-based pellets, a thin layer of Au is sputtered onto both sides of the pellets to form a configuration of Au/LLZT/Au, which is then subjected to EIS tested. As for the Li/LLZT/Li or Li/CF-LLZT/Li symmetric cells, EIS measurements are also carried out to

evaluate the interface resistances. X-ray photoelectron spectroscopy (XPS) was performed on the Thermo Scientific Nexsa using 72 W monochromatic Al Kα radiation. The 400 □m X-ray spot was used for selected area XPS analysis. The base pressure in the analysis chamber was about 3×10^{-9} mbar. Typically, the hydrocarbon C1s line at 284.8 eV from adventitious carbon is used for energy referencing.

As for characterizations such as XRD, ToF-SIMS and Raman, the samples are firstly sealed in a centrifuge tube by parafilm in the glove box, and then transferred to the testing chambers for further analysis. The special transfer tool is employed during our XPS test. It is a home-made device (Figure S0) which is capable of protecting sample from air exposure and is compatible with the XPS apparatus.

Figure S0: The home-made XPS transfer chamber

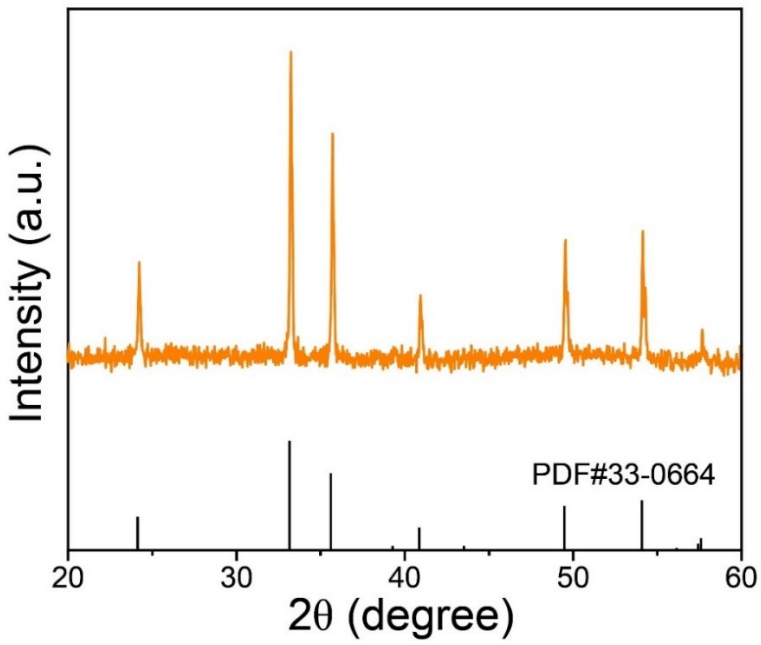

Figure S1: XRD pattern of pyrolysis product of polymer-$Fe(NO_3)_3$ layer. The product was prepared according to the following procedure: A precursor solution containing 50 mM $Fe(NO_3)_3$ and 50 mg/mL PAA dissolved in isopropanol is dispensed into an aluminum trioxide crucible. Upon complete evaporation of the isopropanol, the crucible is transferred to a tube furnace, where the pyrolysis process is carried out under identical conditions to those used for preparing the Fe_2O_3 nanofilm on the ZrO_2 substrate.

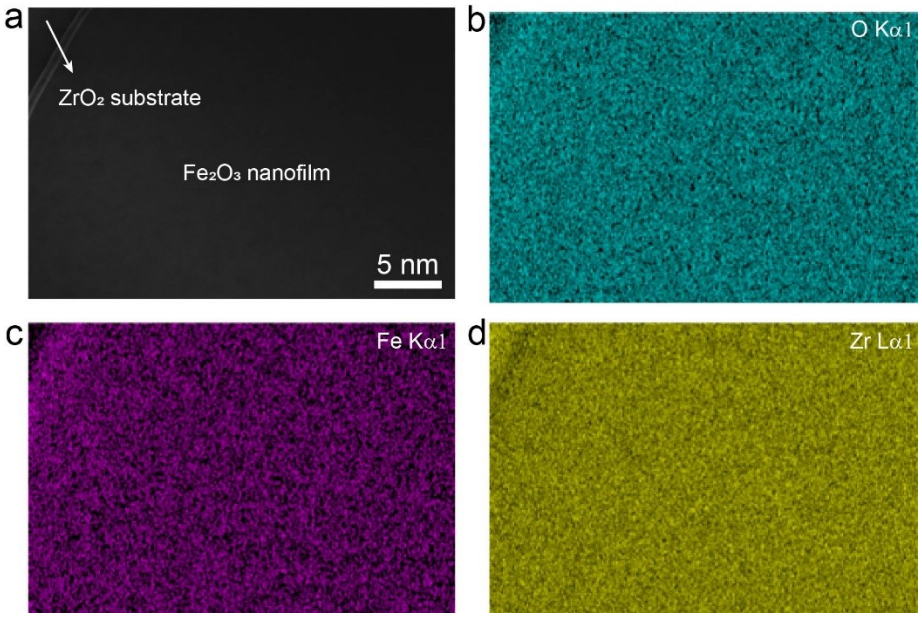

Figure S2: (a) The SEM image of Fe_2O_3 nanofilm coated on ZrO_2 substrate through a polymer assisted process; The image of edge of Fe_2O_3 nanofilm and ZrO_2 substrate is captured in order to show more details; The corresponding element distribution mapping of O (b), Fe (c) and Zr (d) are also presented.

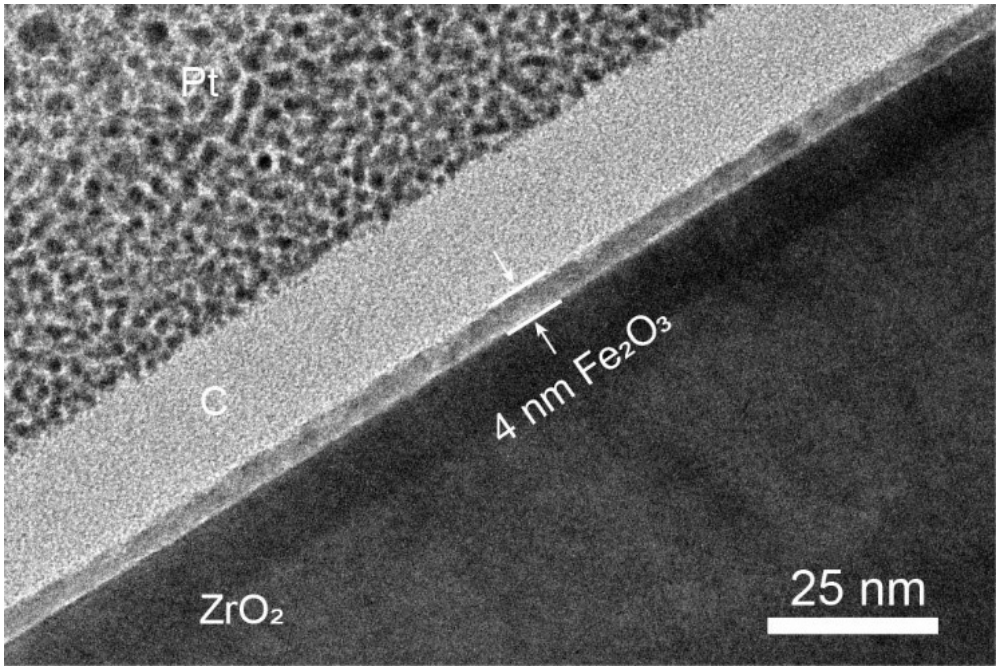

Figure S3: TEM image of 4 nm Fe_2O_3 nanofilm by solution-based method.

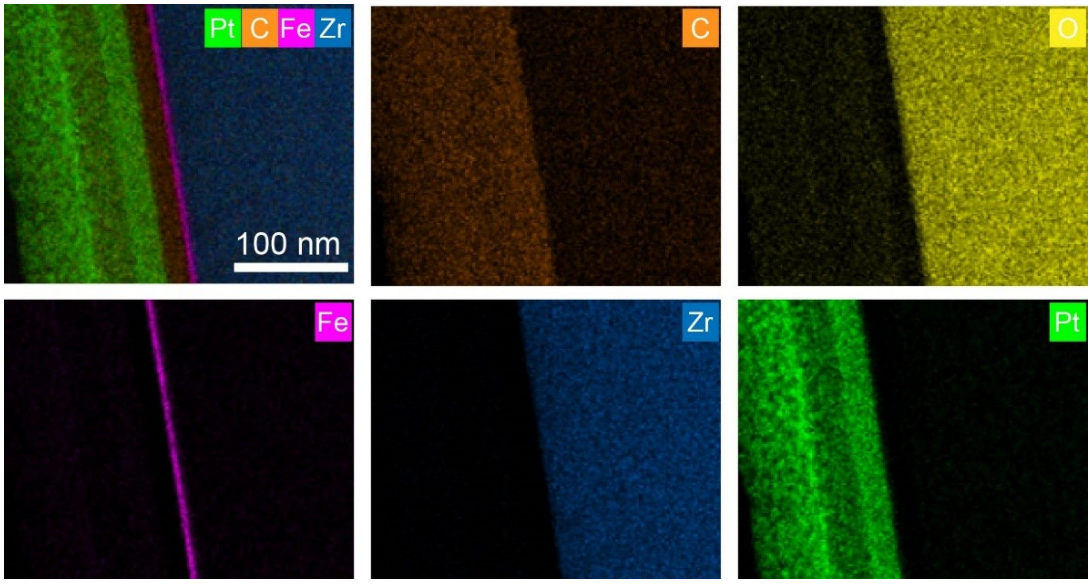

Figure S4: EDS elemental mappings of the 4 nm Fe_2O_3 nanofilm.

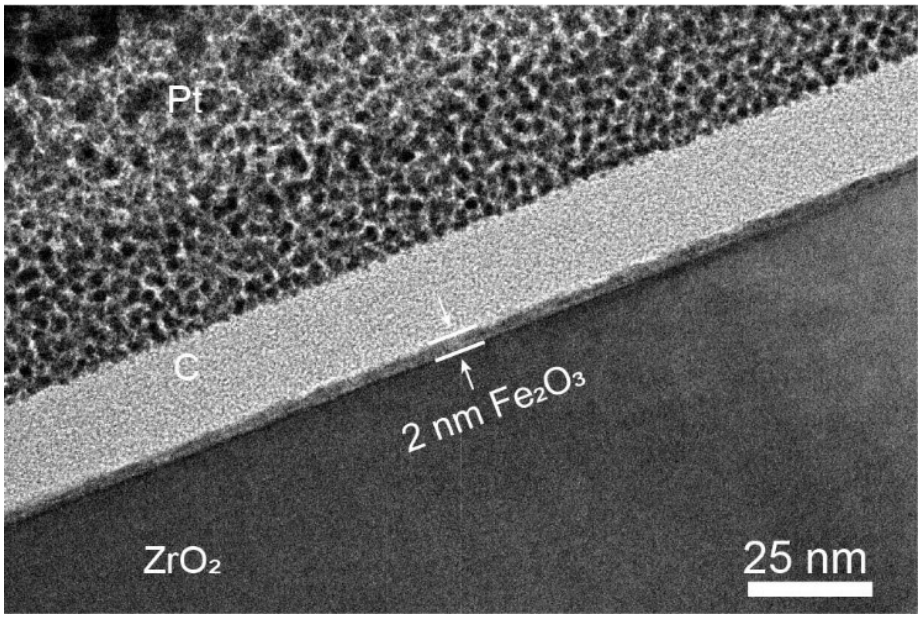

Figure S5: TEM image of 2 nm Fe_2O_3 nanofilm by solution-based method.

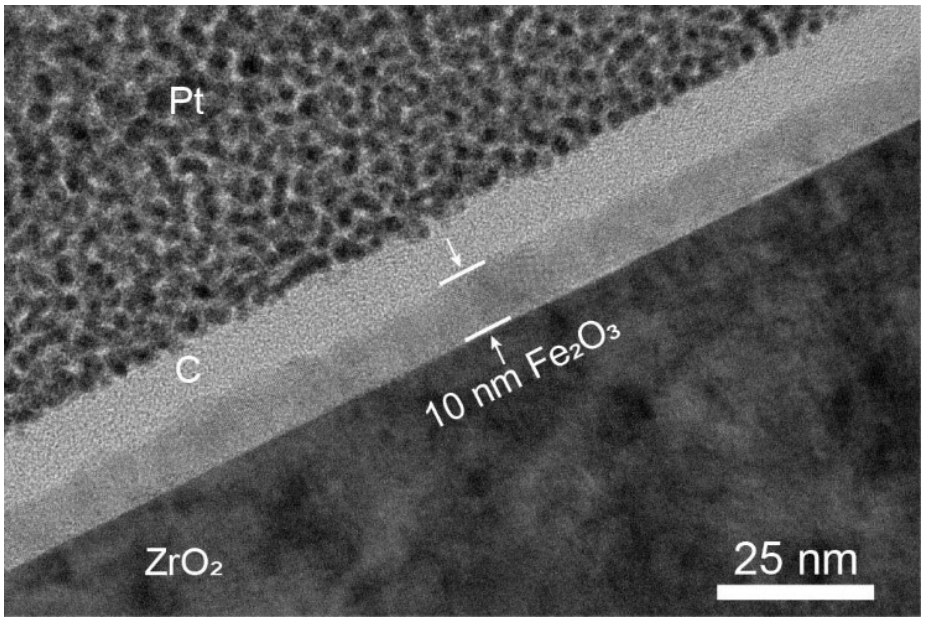

Figure S6: TEM image of 10 nm Fe_2O_3 nanofilm by solution-based method.

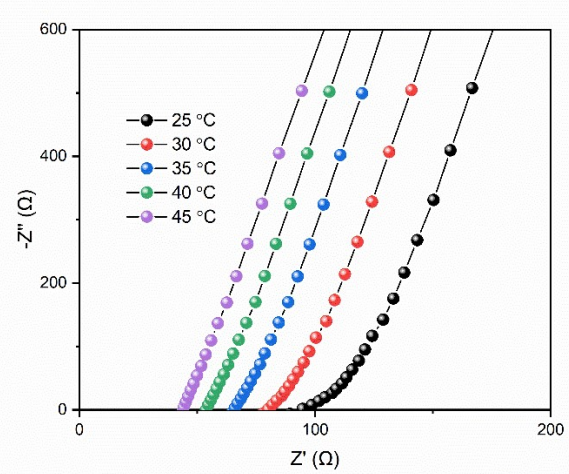

Figure S7: Electrochemical impedance spectroscopy (EIS) of LLZT pellets at the temperature from 25-45 °C.

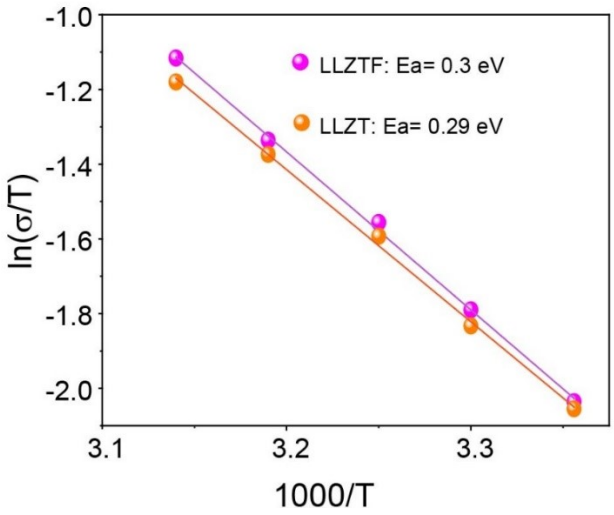

Figure S8: Arrhenius plots of the LLZT pellet and CF-LLZT pellet ionic conductivity.

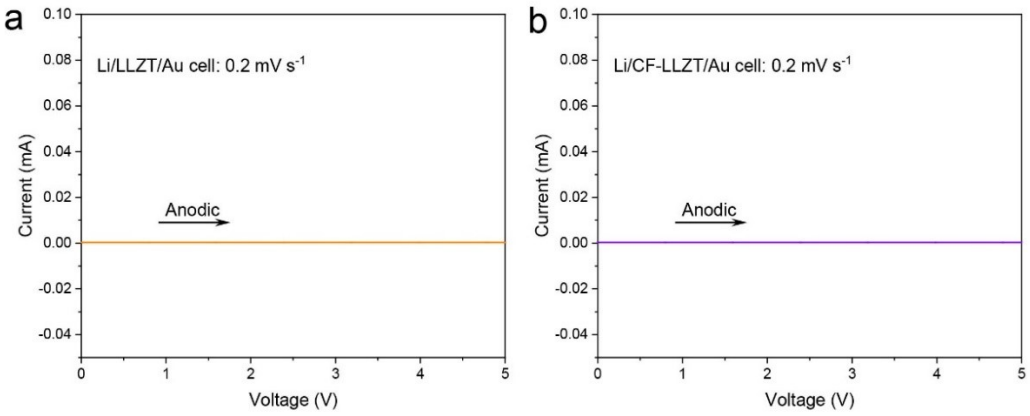

Figure S9. Linear sweep voltammetry for the Li/LLZT/Au cell (a) and the Li/CF-LLZT/Au cell (b) with a scan rate of 0.2 mV s^{-1} between 0 V and 5.0 V.

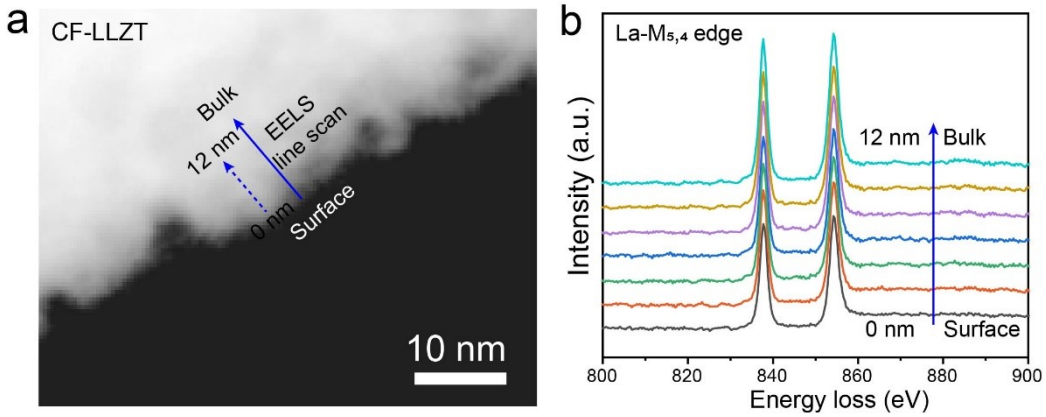

Figure S10: (a) Cross-sectional DF-STEM image of CF-LLZT. The blue solid arrow embodies the direction of EELS line scan from surface (0 nm) to bulk (12 nm). The EELS spectra of the (b) La-$M_{5,4}$ edge in the selected region in the STEM image.

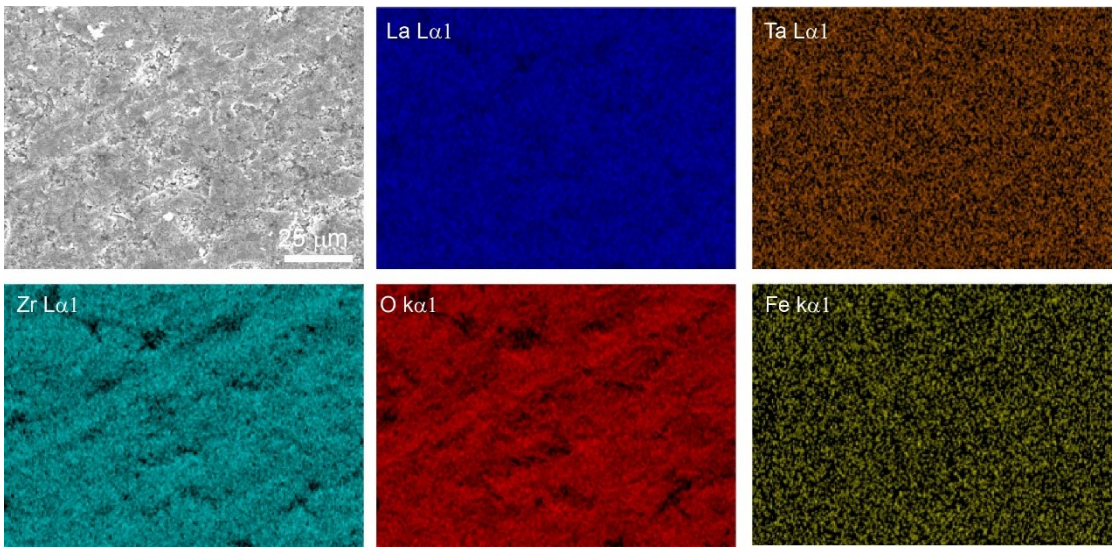

Figure S11: EDS elemental mappings of CF-LLZT.

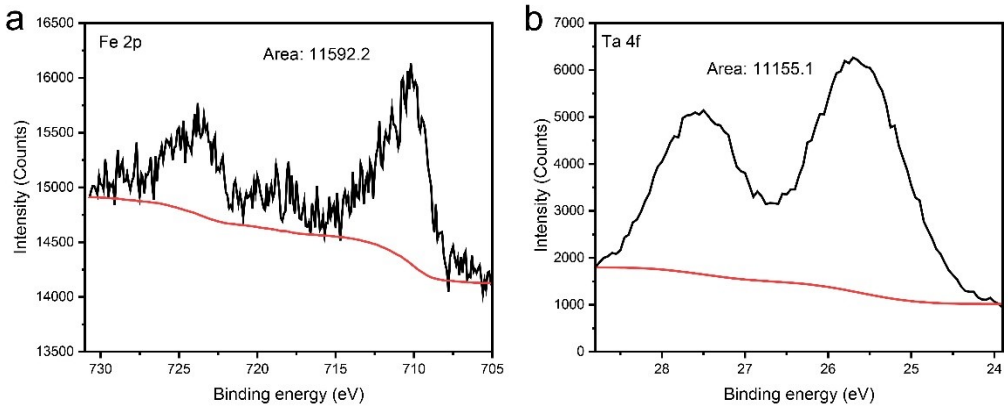

Figure S12: (a) Fe 2p and (b) Ta 4f narrow-range spectra.

The XPS narrow-range spectra of Fe 2p and Ta 4f in CF-LLZT are obtained and analyzed using the

software of Avantage, a professional XPS data processing tool. The background line is added using the Shirley method (red curves) as shown in Figure S9. The software automatically calculated the area of the enclosed curve, with the total area corresponding to the element content in the sample. However, to accurately compare the contents of different elements, the atomic sensitivity factor for X-rays must be considered, and then the values of Area/atomic sensitivity factor of X-ray[1] is used for comparison. The atomic sensitivity factor for X-rays is summarized in the XPS instrument user guidelines and also can be obtained in the reported literature.[2] Here, we use the equation 1 to compare the Fe/Ta ratio in the crust of CF-LLZT. The atom ratio of Fe and Ta can be calculated by the following equation:

$$Atom1{:}Atom2 = \frac{Area1 \Big/ atomic\ sensitivity\ factores\ for\ X\text{–}ray}{Area2 \Big/ atomic\ sensitivity\ factores\ for\ X\text{–}ray} \qquad \text{Equation 1}$$

The atom ratio of Fe and Ta= $\frac{11592.2 \Big/ 1.82}{11155.1 \Big/ 1.69} \approx 1$

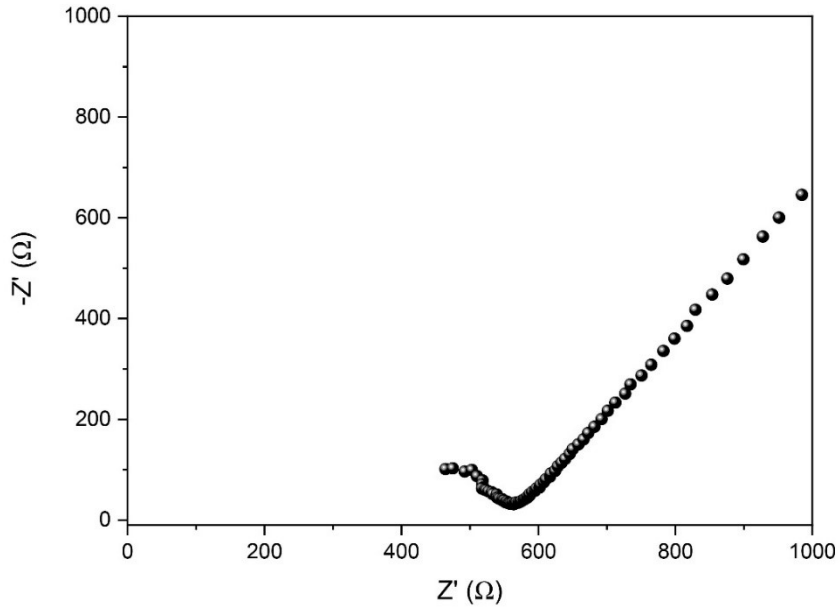

Figure S13: EIS of $Li_5Fe_{0.5}La_3Zr_{1.5}Ta_{0.5}O_{12}$ pellet and Li^+ conductivity is 0.08 mS cm^{-1} calculated by the equation of $\sigma = \frac{l}{RS}$.

Table S1: Rietveld refinement result of $Li_5Fe_{0.5}La_3Zr_{1.5}Ta_{0.5}O_{12}$

Sample		**Site**	**Atom**	**x**	y	**z**	Atom	Occupancy
	Phase:Ia-3d	24	La	0.125	0	0.250	La	1
	a=12.9365895 Å	16	Zr/Ta	0	0	0	Zr	0.75
		16	Zr/Ta	0	0	0	Ta	0.25
$Li_5Fe_{0.5}La_3Zr_{1.5}Ta$	V=2165.00744 Å^3	24	Li1	0.375	0	0.250	Li	0.5386

$_{0.5}O_{12}$	R_{wp}=13.22%						Fe	0.0561
	R_p=9.64%	96	Li2	0.093	0.688	0.593	Li	0.3912
	GOF=3.12						Fe	0.014
		96	O	-0.0312	0.0555	0.156	O	1

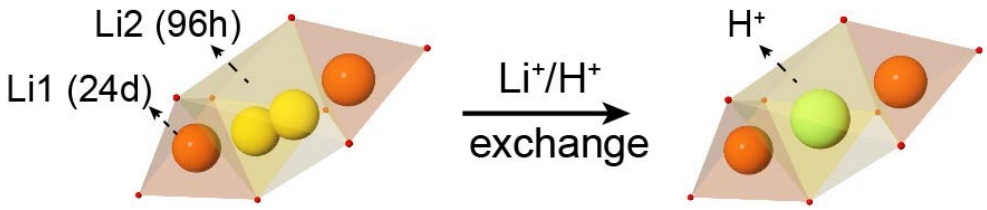

Figure S14: Schematic illustrations of structural in LLZT before and after Li^+/H^+ exchange. Proton can occupy Li2 (96h) and impede lithium-ion transmission.

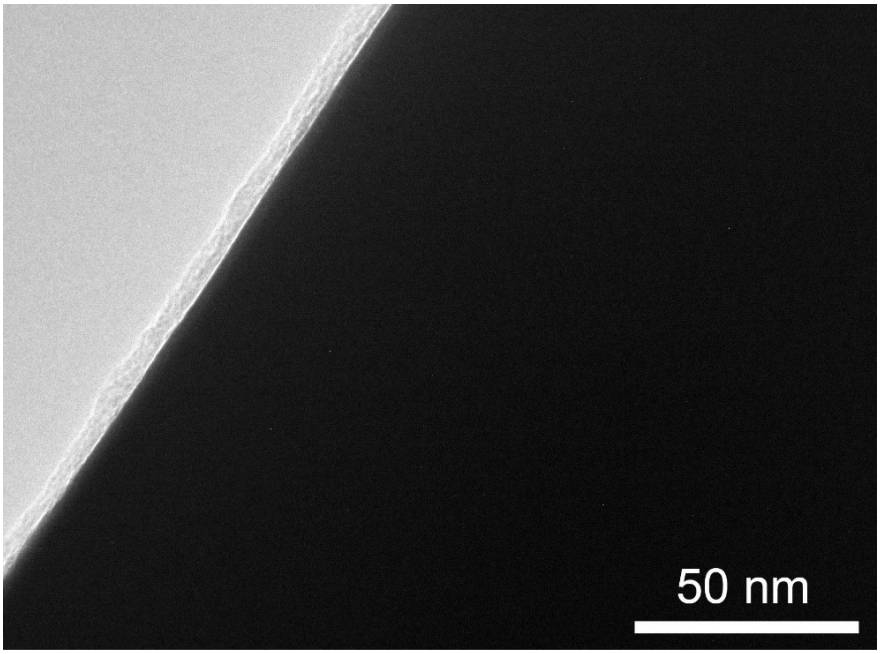

Figure S15: TEM image of LLZT particle and a Li_2CO_3 nanolayer generates on its surface.

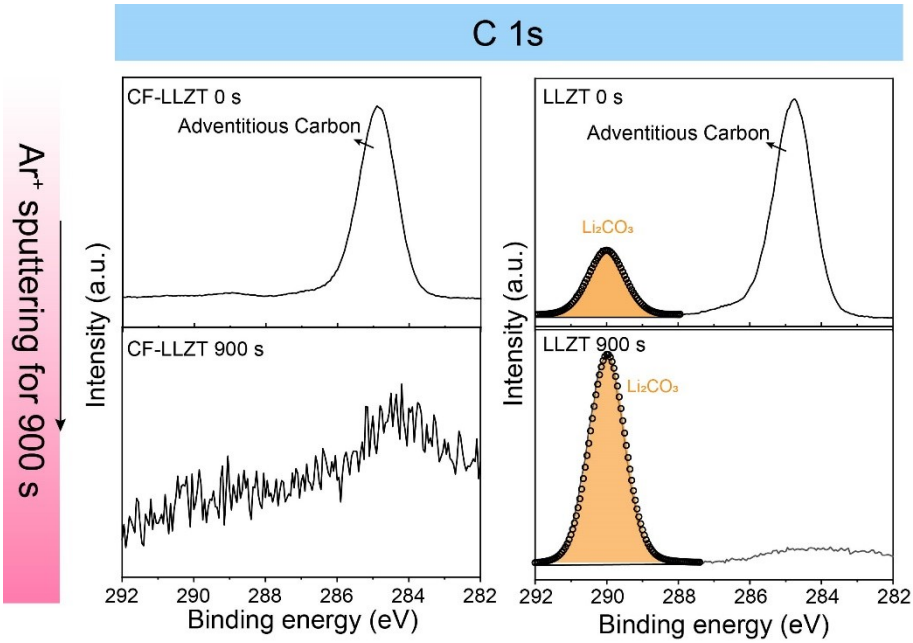

Figure S16: XPS spectra of C 1s for CF-LLZT and LLZT before and after 900s sputtering by Ar^+.

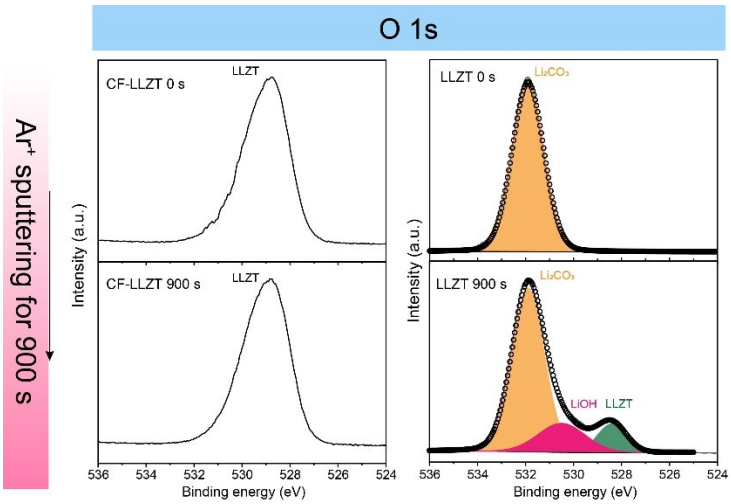

Figure S17: XPS spectra of O 1s for CF-LLZT and LLZT before and after 900s sputtering by Ar^+.

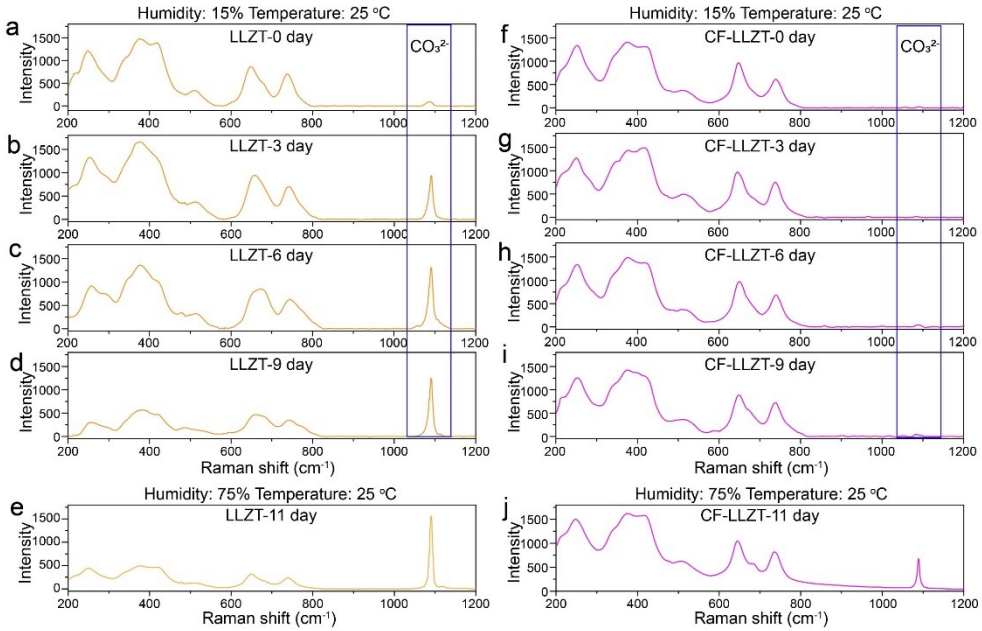

Figure S18: The Raman spectra of LLZT with the exposure time at 0 (a), 3 (b), 6 (c), 9 (d) and 11 (e) days; The Raman spectra of CF-LLZT with the exposure time at 0 (e), 3 (f), 6 (g), 9 (i) and 11 (j) days. The humidity had been controlled at ~ 15% during the exposure time of 9 days and it is increased to 75% on 10th and 11th days with the temperature of 25 °C.

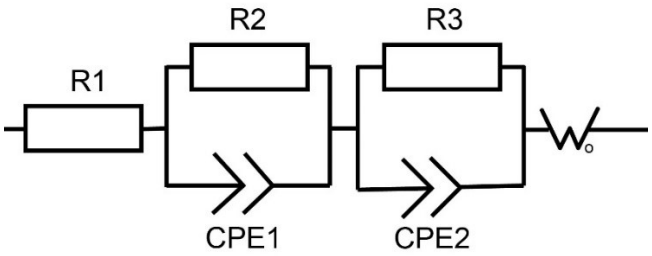

Figure S19: The equivalents circuit modeled used for fitting Li/CF-LLZT/Li EIS data.

Table S2. Electrochemical impedance for typical as-assembled Li/CF-LLZT/Li with varying doping amount of Fe element at 25 °C. Equivalent circuit modeling of the measured Nyquist plots is used to obtain the resistance value of each component.

Li symmetric cell	**Bulk ASR (Ω cm^2)**	**Grain boundary ASR (Ω cm^2)**	**Total Interfacial EIS ASR (Ω cm^2)**	**Interfacial EIS ASR (Ω cm^2)**
CF-LLZT-2 nm	39	30	31	15.5
CF-LLZT-4 nm	41	28	12	6
CF-LLZT-10 nm	49	50	278	139

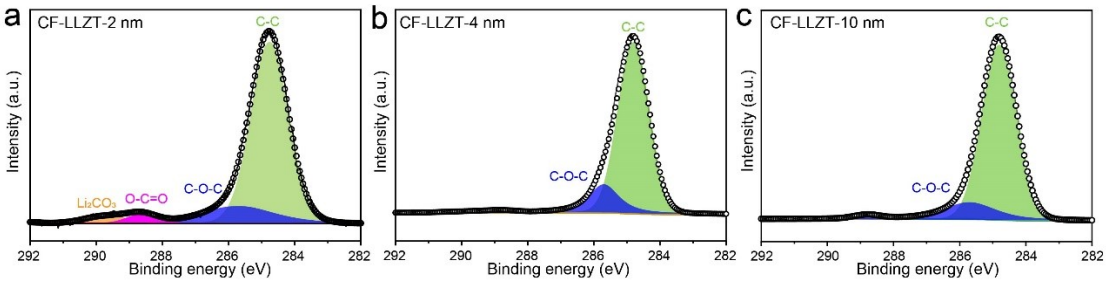

Figure S20: XPS C1s spectrum of CF-LLZT-2 nm (a), CF-LLZT-4 nm (b) and CF-LLZT-10 nm (c). A minimal amount of lithium carbonate is detected on the surface of CF-LLZT-2 nm.

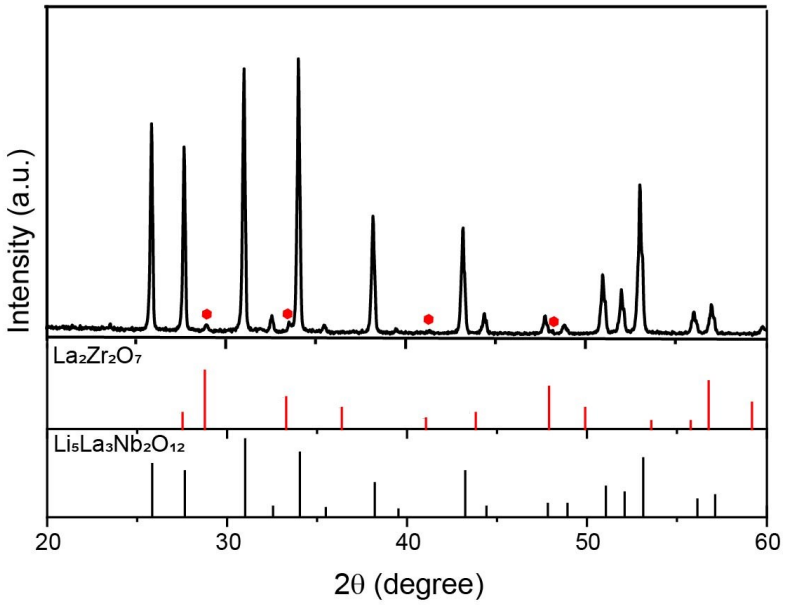

Figure S21: XRD patterns of a sintered sample with fivefold iron ion modified on the surface of an LLZT pellet compared to CF-LLZT-10 nm. The new phase of $La_2Zr_2O_7$ appear in the pattern and marked as hexagonal in the pattern. The sample is prepared by the following process: A 30 μL precursor solution (0.5 M $Fe(NO_3)_3$ and 100 mg/mL PAA dissolved in isopropanol) is dripped onto LLZT pellets, and a spin-coating process is conducted with key parameters set at 5000 rpm for 30 s using a Laurell spin-coater at room temperature. Subsequently, the modified pellets are transferred into a tube furnace for a sintering process at 750 °C with an increasing rate of 5 °C/min in an oxygen atmosphere for 2 h.

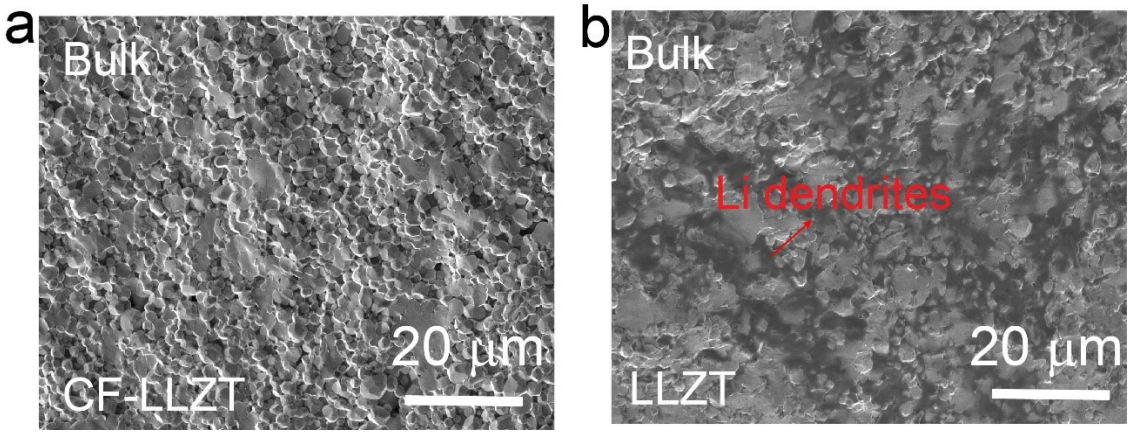

Figure S22. The SEM sectional images of CF-LLZT bulk (a) and LLZT bulk (b) after long-term cycling of symmetric cell. After disassembling the cells, the cross section of SSEs is achieved by frustration with the use of a thin-tipped tweezer.

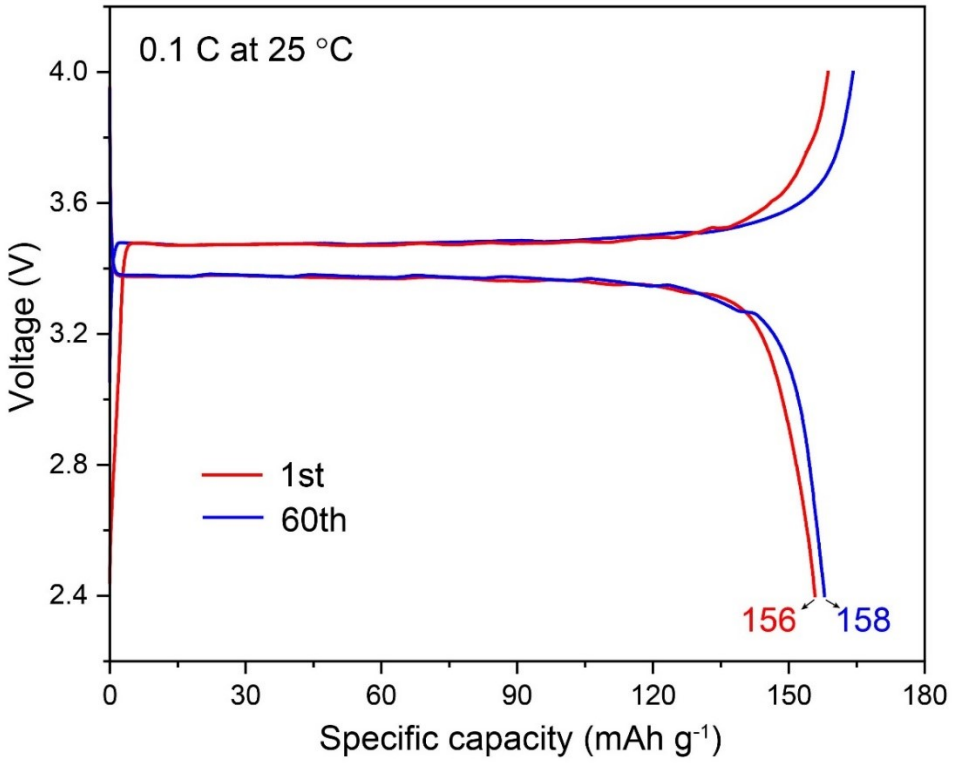

Figure S23: The charge and discharge curves of Li/CF-LLZT/Li at 0.1 C before (red curves) and after (blue curves) rate testing.

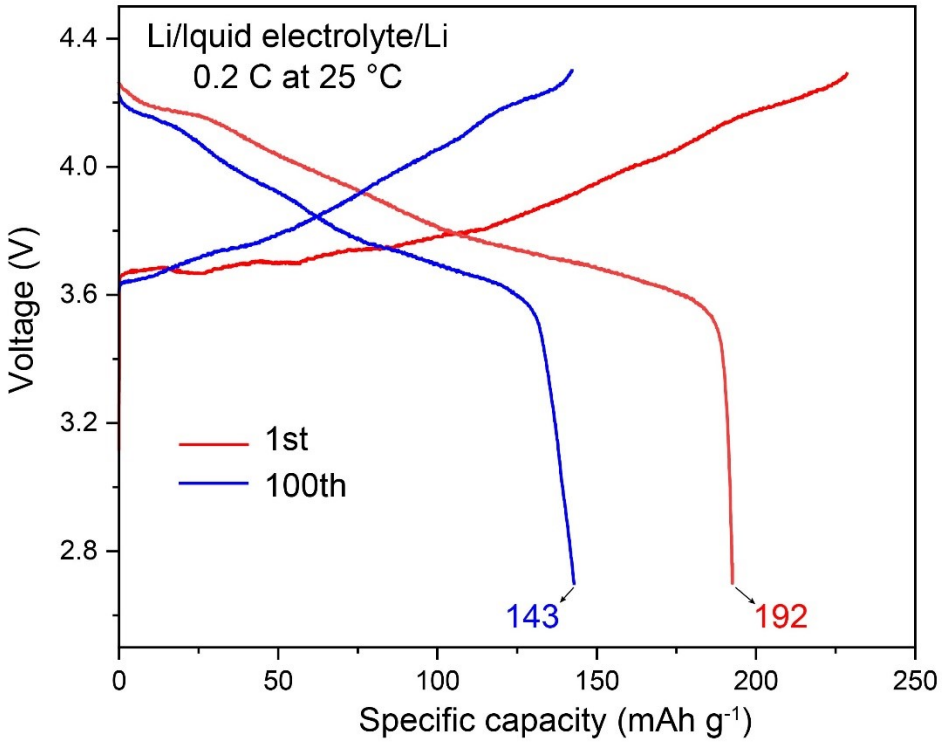

Figure S24: The charge and discharge curves of Li/liquid electrolyte/Li at 1st and 100th cycles under the current density of 0.2 C.

Reference:

1. A. Jablonski, B. Lesiak, L. Zommer, M. F. Ebel, H. Ebel, Y. Fukuda, Y. Suzuki and S. Tougaard, Surf. Interface. Anal., 2004, 21, 724-730.
2. Chastain J, King Jr R C. Handbook of X-ray photoelectron spectroscopy[J]. Perkin-Elmer Corporation, 1992, 40: 221.